Active Site Contacts in the Purine Nucleoside Phosphorylase−Hypoxanthine Complex by NMR and *ab Initio* Calculations†

Hua Deng,*,‡ Sean M. Cahill,‡ José-Luis Abad,§ Andrzej Lewandowicz,‡ Robert H. Callender,‡ Vern L. Schramm,‡ and Roger A. Jones§

Department of Biochemistry, Albert Einstein College of Medicine, 1300 Morris Park Avenue, Bronx, New York 10461, and Department of Chemistry, Rutgers, The State University of New Jersey, Piscataway, New Jersey 08854

Received August 25, 2004; Revised Manuscript Received October 6, 2004

ABSTRACT: Hypoxanthine (Hx) with specific ^{15}N labels has been used to probe hydrogen-bonding interactions with purine nucleoside phosphorylase (PNP) by NMR spectroscopy. Hx binds to human PNP as the N-7H tautomer, and the N-7H ^{1}H and ^{15}N chemical shifts are located at 13.9 and 156.5 ppm, respectively, similar to the solution values. In contrast, the ^{1}H and ^{15}N chemical shifts of N-1H in the PNP·Hx complex are shifted downfield by 3.5 and 7.5 ppm to 15.9 and 178.8 ppm, respectively, upon binding. Thus, hydrogen bonding at N-1H is stronger than at N-7H in the complex. Ab initio chemical shift calculations on model systems that simulate Hx in solution and bound to PNP are used to interpret the NMR data. The experimental N-7H chemical shift changes are caused by competing effects of two active site contacts. Hydrogen bonding of Glu201 to N-1H causes upfield shifts of the N-7H group, while the local hydrogen bond (C═O to N-7H from Asn243) causes downfield shifts. The observed N-7H chemical shift can be reproduced by a hydrogen bond distance ∼0.13 Å shorter (but within experimental error) of the experimental value found in the X-ray crystal structure of the bovine PNP·Hx complex. The combined use of NMR and ab initio chemical shift computational analysis provides a novel approach to understand enzyme−ligand interactions in PNP, a target for anticancer agents. This approach has the potential to become a high-resolution tool for structural determination.

Purine nucleoside phosphorylase (PNP)[1] catalyzes the reversible phosphorolysis of the N-ribosidic bond of 6-oxypurine nucleosides and deoxynucleosides (Scheme 1). In humans, the metabolic role of PNP is to remove deoxyguanosine that accumulates from DNA turnover. The genetic deficiency of PNP causes a T-cell immunodeficiency due to dGTP accumulation specifically in dividing T-cells (*1*). Inhibition of PNP inhibits the growth of activated T-cells, providing a clinical means to ameliorate T-cell proliferative disorders (*2*). The catalytic acceleration of PNP is achieved through formation of a transition state with oxacarbenium ion character and specific leaving group interactions to the purine. Ribosides with better leaving groups such as 4-nitrophenyl β-D-riboside are poor substrates (*3*). Catalytic site contacts to the purine hold it in place to facilitate ribosyl electrophile migration from the leaving group to a phosphorus nucleophile also immobilized at the catalytic site (*4*). Although the reaction equilibrium favors nucleoside synthesis, the enzyme in vivo operates in the phosphorolysis direction because of the rapid metabolic removal of the products by purine phosphoribosyltransferases. Bovine PNP binds tightly to hypoxanthine (∼2 pM) generated from inosine in the absence of PO_4 (*5*). Thus the unique leaving interactions of catalysis also contribute to hypoxanthine binding.

Hydrogen bond interactions at the enzyme active site are important to understand PNP catalysis. Short, strong hydrogen bond interactions at an enzyme active site often result in the detection of isolated NH and OH proton resonances in the downfield region of the proton NMR spectrum [>16 ppm (*6*−*10*)]. These resonances, when assigned, can be used to determine the hydrogen-bonding distances quantitatively by using the correlation between chemical shifts and hydrogen-bonding distances (*10, 11*) and by fractionation factor measurements (*6, 12*−*15*). However, when the resonances are not located far downfield, the determination of the hydrogen-bonding distance may be difficult because factors other than the local hydrogen bonding may become important for the proton chemical shift values, and spectral overlap may prevent the fractionation factor measurements. Hydrogen bond interactions at the active site of hPNP with the transition state analogue immucillin-H (ImmH) results in two new downfield NH proton resonances at 14.9 and 12.7 ppm. These have been assigned to the N-1H and N-7H of ImmH, respectively (*16*). However, estimates of the hydrogen bond distances based on these NH resonances were not made due to the difficulties mentioned above. Furthermore, since the N-7H resonance overlaps with another protein resonance, a fractionation factor measurement is not feasible.

† Supported by Research Grants GM068036, EB001958 (R.H.C.), GM41916 (V.L.S.), and EB002809 (R.A.J.) from the NIH.

* Address correspondence to this author: 718-430−2437 (phone); 718-430-8565 (fax); hdeng@aecom.yu.edu (e-mail).

‡ Albert Einstein College of Medicine.

§ Rutgers, The State University of New Jersey.

[1] Abbreviations: hPNP, human purine nucleoside phosphorylase; Hx, hypoxanthine; ImmH, immucillin-H; HMQC, heteronuclear multiple-quantum coherence; HSQC, heteronuclear single-quantum coherence; TSP, perdeuterated 3-(trimethylsilyl)propionate sodium salt.

10.1021/bi048167i CCC: $27.50
Published on Web 11/24/2004

Scheme 1: Reactions Catalyzed by PNP[a]

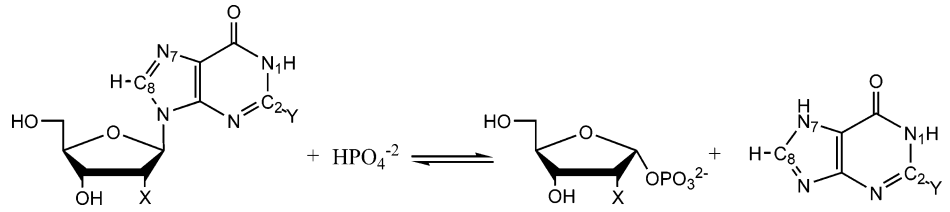

[a] X = H or OH; Y = H or NH_2.

In this study, we have extended our NMR measurements to the hPNP·Hx complex containing Hx with uniform or specific ^{15}N labels. The proton and ^{15}N chemical shifts of the two Hx NH groups in solution and in an enzyme complex have been analyzed by ab initio chemical shift calculations to determine if it is possible to interpret the experimental data quantitatively in terms of hydrogen bond distance.

Ab initio NMR chemical shift calculations have been used extensively for ^{15}N and ^{13}C to correlate the observed chemical shifts with molecular structures and environments (for a recent review, see ref *17*). It has been found that $^{15}N^{H}$ chemical shifts are sensitive to the molecular conformation as well as to hydrogen bonding and electrostatics (*18*, *19*). To reproduce the experimentally observed ^{15}N chemical shifts, it is essential to include the hydrogen-bonding partners in the calculation models (*19*−*21*). Previous ab initio ^{1}H chemical shift calculations also suggest that the effect of hydrogen bonding on $^{1}H^{N}/^{1}H^{O}$ chemical shifts is particularly significant (*18*, *22*). Here we use ab initio ^{1}H and ^{15}N NMR chemical shift calculations for several Hx model systems to simulate environments in solution and bound at the active site of PNP. When judged by the relative chemical shift changes of Hx in different environments, the results from experiments and calculations are in good agreement. Thus, the quantum chemical methods appear to be sufficiently accurate to provide a quantitative interpretation of the proton chemical shift changes for a small rigid molecule such as Hx, when proper models are used. Theoretical analysis of our NMR data provided an interpretation of the Hx N-1H and N-7H chemical shift changes at the active site of hPNP that is different from that previously made. These findings can be used to refine the structure of active site contacts determined from X-ray crystallographic studies.

MATERIALS AND METHODS

[U-^{15}N]Adenosine was purchased from Spectra Stable Isotopes. The [^{15}N-1]Hx, [^{15}N-3]Hx, and [^{15}N-7,^{13}C-8]Hx were synthesized as reported previously (*23*, *24*). [U-^{15}N]-Hx was made from [U-^{15}N]adenosine by enzymatic reaction using adenosine deaminase and then nucleoside hydrolase, followed by purification with HPLC using a Waters C18 column. Human PNP was prepared as described previously (*16*). The concentration of Hx was determined by its extinction coefficient of 10.7 mM^{-1} cm^{-1} at 250 nm, pH 6. Complexes of hPNP·Hx were prepared by mixing hPNP and the purine at a concentration ratio of 1:1.2, and the complexes were washed three times in a Centricon-100 with 10 volumes of 0.5 M NaCl at pH 6.5, so that the final free inhibitor concentration was less than 0.1% of the protein concentration. The concentration of the enzyme was typically 1.0−1.5 mM. D_2O (5%) was added to all hPNP samples in aqueous solution to provide a lock signal for NMR experiments.

Solution NMR measurements for proteins, substrates, and protein−ligand complexes were conducted on Bruker DRX300 and Varian Inova 600 spectrometers. One-dimensional proton spectra for protein samples in aqueous solution were typically collected using jump−return water suppression (*25*) using 512 scans, a sweep width of 30 ppm sampled with 16K points, and a recycle delay of 1.5 s. The jump−return delay was adjusted so that the maximum excitation was at ∼15 ppm. The 1D difference spectra of hPNP·Hx complexes containing ^{15}N-labeled Hx were obtained by positioning the carrier of the ^{15}N decoupling pulse within and outside of the ^{15}N spectral region and by shifting the receiver phase by 180 deg during alternative scans (*26*). This method was found to be significantly more sensitive than the method based on HMQC when transverse relaxation of the resonances was very fast. Two-dimensional $^{1}H-^{15}N$ HMQC spectra for the hPNP·[U-^{15}N]Hx complex were acquired with the jump−return pulse and the refocusing delay in the pulse sequence just before acquisition was eliminated to reduce the signal loss due to relaxation, and no decoupling was applied during acquisition. This method worked on hPNP samples (∼100 kDa) when TROSY and HSQC did not. In theory, splitting in the ^{1}H dimension with an antiphase pattern should be observed for each ^{15}N signal. However, due to the constructive and destructive interference of dipole−dipole and chemical shift anisotropy, the relaxation of one component is much faster than the other even at 600 MHz (cf. ref *27*), and only one component of the doublet was detected. The 2D HMQC spectrum was collected with 2K and 32 complex points in t_2 (^{1}H) and t_1 (^{15}N), respectively, with 256 scans per t_1 point and a recycle delay of 1.5 s. The value of t_{1max} was set to 2.6 ms, and t_{2max} = 170 ms. A cosine bell window function was applied to the proton dimension in data processing and in the ^{15}N dimension; the data were linearly predicted to 128 points and zero filled to 256 points before processing with a cosine bell window function. A sensitivity-enhanced HSQC 2D $^{1}H-^{15}N$ experiment that was optimized for either single (J_{NH} = 105 Hz) or two ($^{2}J_{NH}$ = 25 Hz) bond correlation was used to record the spectra of [U-^{15}N]Hx in 55:45 (v/v) DMSO-d_6/acetonitrile-d_3 at −40 °C. The solubility of Hx in acetonitrile is significantly less than in DMSO. It was used only for the purpose that the NMR measurements can be performed at temperatures lower than 18 °C. In these measurements, the t_{1max} in the ^{15}N dimension was increased to 23.5 ms with 200 data points and 8 scans for each point. Data in the ^{15}N dimension was linearly predicted to 512 points before processing with a cosine bell window function. Proton chemical shifts were referenced to TSP externally at 0.0 ppm.

Ab initio ^{1}H and ^{15}N chemical shielding tensor calculations were made on model systems using the GIAO method as implemented in the Gaussian 98 package (*28*). The calcula-

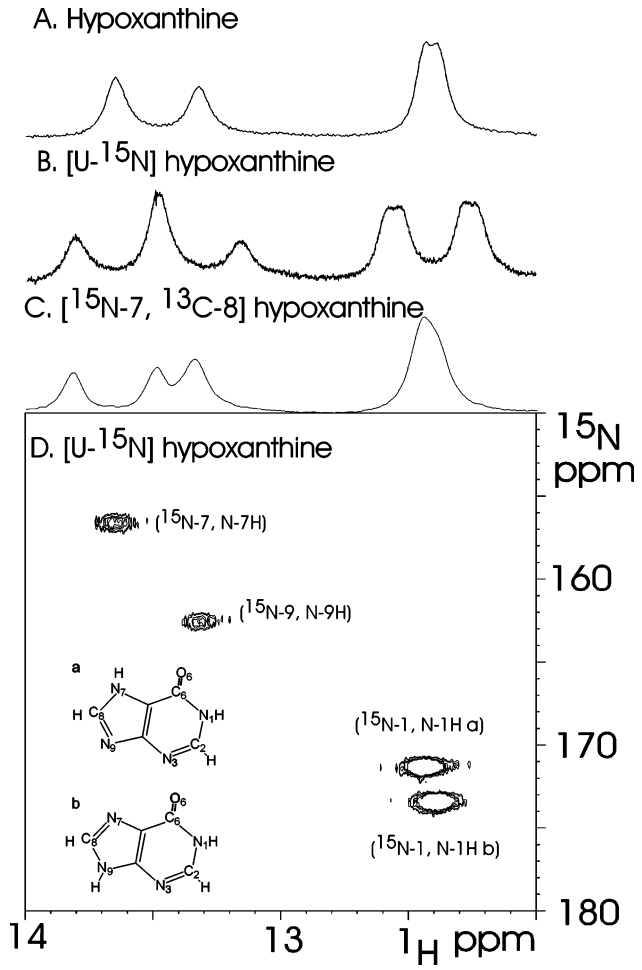

FIGURE 1: NMR spectra for Hx with and without isotopic labels: (A) Hx proton spectrum; (B) [U-^{15}N]Hx proton spectrum; (C) [^{15}N-7,^{13}C-8]Hx proton spectrum; (D) ^{1}H−^{15}N HSQC spectrum of [U-^{15}N]Hx. All samples were prepared in 55% DMSO/45% acetonitrile. The concentration was 4 mM, and the temperature was −40 °C for all samples. The data were obtained on a Bruker DRX300 spectrometer. Other experimental details are described in Materials and Methods.

tions were carried out at the DFT B3LYP level of theory with the 6-311(d,p) basis set. Geometries were first optimized at the same level of theory but with either 6-311(d,p) or 6-31(d,p) basis sets. In general, the calculated isotropic chemical shielding values can be converted to chemical shift values observed in solution NMR experiments by a linear scaling procedure for a better fit (*18*, *29*−*31*). Since our goal is to model the chemical shift changes of a molecule under different environments, we did not use this scaling scheme because we have too few data points to derive parameters that can be used generally. We subtracted the calculated isotropic shielding values from a constant to convert them to chemical shift values so that they can be compared with the experimentally determined chemical shifts. The constant was 32 for ^{1}H and 225 for ^{15}N.

RESULTS

NMR Studies of Hx in Solution. At −40 °C and in a mixture of 55% DMSO/45% acetonitrile, the NMR NH proton resonances of Hx are well isolated (Figure 1A), suggesting that the NH protons are in slow exchange with each other among different tautomers. The spectra of [U-^{15}N]-Hx (Figure 1B) and [^{15}N-7,^{13}C-8]Hx (Figure 1C) clearly show that the most downfield proton resonance at 13.7 ppm is from N-7H. Measurements on the [^{15}N-1]Hx (data not shown) indicate that the resonances near 12.4 ppm are from N-1H of Hx. Thus, the resonance at 13.3 ppm can be assigned to N-9H. The intensity ratios of the N-7H and the N-9H resonances in the Hx 1D spectrum ranged from 53:47 to 57:43 under different temperatures (−40 to 5 °C at pH 5 ± 1 when dissolved in water), suggesting that the relative population ratio of the two tautomers should be close to 55:45. The temperature dependence of all NH chemical shifts was the same, ∼+0.12 ppm from −40 to 5 °C for the same sample. The population ratio determined here is consistent with the 58:42 ratio determined by indirect ^{13}C NMR measurements in an earlier study on Hx in 100% DMSO (*32*). The ^{1}H−^{15}N HSQC spectrum of the [U-^{15}N]Hx (Figure 1D) reveals that the ^{15}N chemical shifts of the N-7H, N-9H, and the two N-1Hs from the two different Hx tautomers are at 156.7, 162.7, 171.2, and 173.3 ppm, respectively. These results also show that the concentrations of other tautomeric forms of Hx are negligible under these experimental conditions.

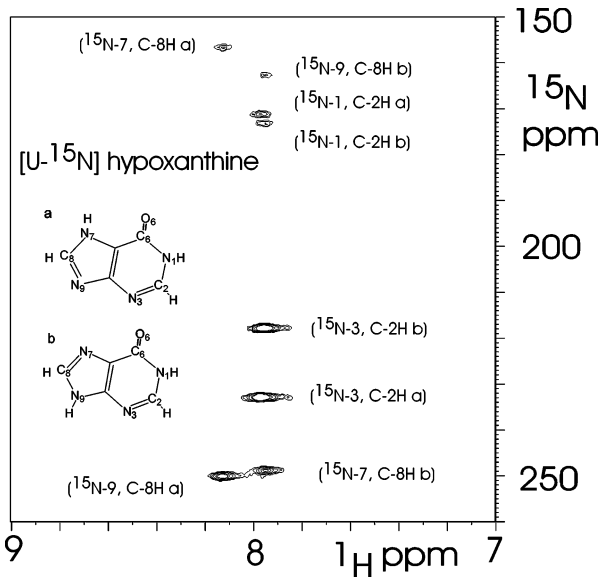

FIGURE 2: ^{1}H−^{15}N long-range HSQC spectrum of [U-^{15}N-7]Hx optimized for two-bond ^{15}N−^{1}H coupling ($^{2}J_{NH}$ = 25 Hz). Other experimental conditions were the same as in Figure 1.

The ^{1}H−^{15}N long-range HSQC spectrum of the [U-^{15}N]-Hx optimized for two-bond ^{1}H−^{15}N coupling is shown in Figure 2. J_{NH} in the HSQC pulse sequence was set to 25 Hz. The ^{15}N resonances between 150 and 180 ppm are from the protonated nitrogens of the two Hx tautomers as shown in Figure 1D. A comparison with measurements on the [^{15}N-7,^{13}C-8]Hx indicates that the ^{15}N chemical shifts of the unprotonated N-7 and N-9 are at 248.7 and 250.0 ppm, respectively. The HSQC spectrum of [^{15}N-3]Hx reveals that the ^{15}N-3 resonances of the two tautomers are at 217.8 and 232.8 ppm, respectively. There is a small but detectable ^{1}H chemical shift difference (∼0.02 ppm) for the C-2H resonances in these two tautomers, and each C-2H resonance links the ^{15}N chemical shifts of the N-1 and N-3 of the same tautomer (Figure 2). The ^{15}N-3 chemical shift of inosine is at 213.0 ppm (data not shown), similar to the upfield ^{15}N-3 resonance at 217.8 ppm for Hx (Figure 2). It is also known that the ^{15}N-3 chemical shift in the N-9 substituted tautomer

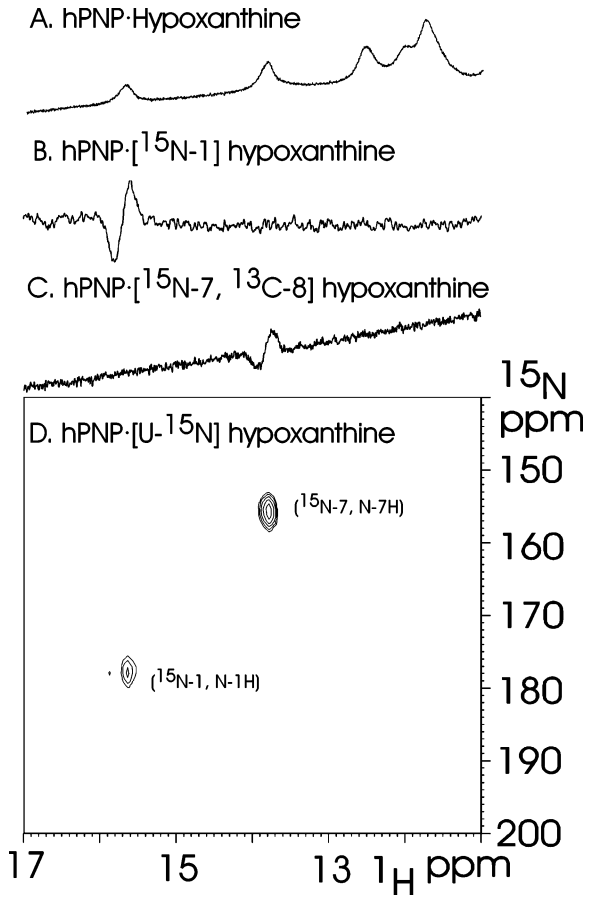

FIGURE 3: NMR spectra for the complex of hPNP·Hx with unlabeled and isotopically labeled Hx: (A) proton spectrum of the hPNP·Hx complex; (B) difference proton spectrum between the hPNP·[^{15}N-1]Hx proton spectrum with and without ^{15}N decoupling during acquisition; (C) difference proton spectrum between the complex of hPNP·[^{15}N-7,^{13}C-8]Hx with and without ^{15}N decoupling during acquisition; (D) jump−return ^{1}H−^{15}N HMQC spectrum of hPNP·[U-^{15}N]Hx. Spectra A and D were obtained on a Varian Inova 600 spectrometer, and spectra B and C were obtained on a Bruker DRX300 spectrometer. The concentration ratio of hPNP to Hx was approximately 1 to 1 with 1 mM concentration of each at pH 6.5 at 25 °C. Other experimental details are described in Materials and Methods.

appears consistently ~20 ppm upfield from the N-7 substituted tautomer in a number of purine derivatives (*33*). Therefore, the 217.8 ppm ^{15}N-3 resonance can be assigned to the N-9H tautomer and the assignments of the rest of the ^{15}N and ^{1}H resonances of Hx can then be completed (Figures 1D and 2).

NMR Studies of Hx in hPNP. Two new proton resonances appear in the downfield region at 15.9 and 13.8 ppm in the NMR spectrum of hPNP·Hx (Figure 3A). They can be assigned to the resonances from the N-1H and the N-7H protons of Hx, respectively, on the basis of measurements of the hPNP·Hx complex with ^{15}N specifically labeled at N-1 (Figure 3B) or N-7 (Figure 3C). Hx is bound to hPNP as the N-7H tautomer. Stronger hydrogen bonding to N-1H in hPNP·Hx than in solution is evident from its 3.5 ppm downfield shift relative to the solution value. The 2D HMQC spectrum of the hPNP·[U-^{15}N]Hx complex (Figure 3D) shows that the ^{15}N-1 chemical shift of Hx is at 178.8 ppm, shifted downfield by 7.5 ppm relative to its solution value (Figure 1D), also consistent with stronger hydrogen bonding to N-1H in the complex. In contrast, the ^{15}N and proton

Chart 1

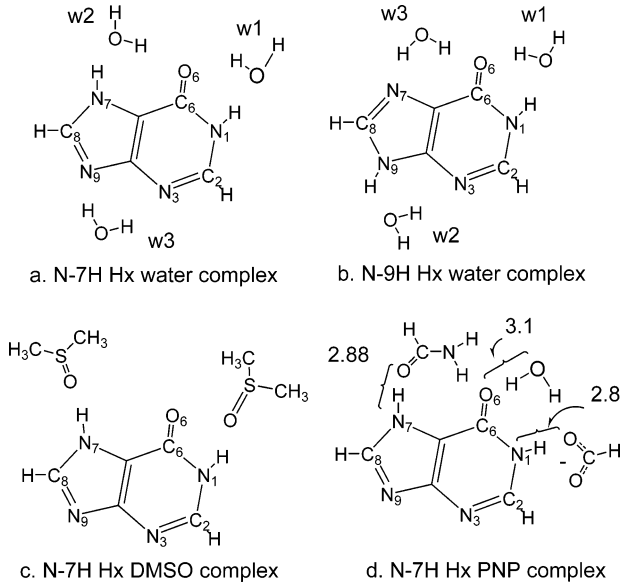

chemical shifts of N-7H change by less than 0.5 ppm upon binding. Normally, such data would be taken to indicate that the hydrogen bonding on N-7H of Hx in the hPNP complex is relatively unchanged from that in organic solvent.

Ab Initio Chemical Shift Calculations. Molecular models for hydrogen bonding in Hx systems include up to three water molecules complexed with each tautomer of Hx (Chart 1, models a and b). The geometries of these model systems were fully optimized (unless indicated otherwise) at the B3LYP/6-311G(d,p) level, and the ^{1}H and ^{15}N isotropic chemical shielding calculations were performed on the optimized geometries using the same basis set. Our interest in the calculations from these model systems is to establish the effects of hydrogen bonding from each water molecule on the ^{1}H and ^{15}N chemical shift values of a given NH group. Thus, only relative chemical shift values are of interest to us.

Comparison of ab Initio and Experimental Chemical Shifts. Calculated chemical shift values of the four protons and four nitrogens for each Hx tautomer complexed with up to three water molecules can be compared to experimental values from Hx in organic solvent (Tables 1 and 2). Such comparisons reveal the follwoing: (1) The ^{1}H chemical shifts of NH groups are very sensitive to the environment so that the order of the relative ^{1}H chemical shift values may change due to external hydrogen bonding. Thus, when studying proton chemical shifts of NH groups, all hydrogen-bonding partners should be included in the model system. (2) The effect of hydrogen bonding on a NH group by a water molecule is mainly local. For example, the ^{1}H and ^{15}N chemical shift changes of the N-1H group induced by the w1 water are nearly the same as the changes induced by three water molecules.

Several qualitative agreements between calculations and experiments are also apparent. For example, the calculated ^{15}N chemical shift of N-3 in N-9H tautomers is consistently >20 ppm upfield compared to the N-7H tautomer under all conditions, consistent with the observation that the upfield N-3 resonance at 217.8 ppm (Figure 2) is due to the N-9H tautomer and also consistent with NMR experiments on N-7

Table 1: Observed and Calculated ^{1}H and ^{15}N Chemical Shifts of Hx N-7H Tautomers[a]

		N-7H Hx					
		experiment		calculated			
nuclei	atom	sol	PNP	vacuum	H_2O (w1)	H_2O (w1+w2)	H_2O (3w)
^{1}H	N-1H	12.4(5)	15.9	7.53	11.55	11.66	11.82
	C-2H	7.9(6)		7.86	7.93	7.97	7.98
	N-7H	13.7	13.9	8.56	8.54	12.67	12.85
	C-8H	8.1(4)		7.72	7.76	7.84	7.86
^{15}N	N-1	171.2	178.8	154.7	157.7	154.6	155.3
	N-3	232.8		239.1	240.2	246.4	237.6
	N-7	156.7	156.5	127.1	125.9	141.4	142.5
	N-9	250.0		262.8	261.9	259.8	250.4

[a] The chemical shifts are in ppm. sol: 55% DMSO/45% acetonitrile. PNP: PNP complex. H_2O(w1): bound with water w1 as shown in Chart 1a. H_2O(w1+w2): bound with water w1 and w2 in Chart 1a. H_2O(3w): bound with all three water molecules in Chart 1a. The last digit in ^{1}H chemical shift observed in solvent is placed in parentheses because their chemical shift values can be of real significance only when they appear in the same spectrum and are used for the purposes of assignment. All structures were optimized before calculations of chemical shifts except the $3H_2O$ complex, which did not achieve convergence so a structure with the lowest energy was selected to calculate the chemical shifts of this complex.

Table 2: Observed and Calculated ^{1}H and ^{15}N Chemical Shifts of the N-9H Hx Tautomers[a]

		N-9H Hx				
		expt	calculated			
nuclei	atom	sol	vacuum	H_2O (w1)	H_2O (w1+w2)	H_2O (3w)
^{1}H	N-1H	12.4	7.54	10.82	10.81	11.22
	C-2H	7.9(4)	7.71	7.79	7.69	7.77
	N-9H	13.3	8.11	8.11	10.89	11.17
	C-8H	7.9(5)	7.50	7.52	7.56	7.63
^{15}N	N-1	173.2	161.2	162.2	161.3	161.4
	N-3	217.8	210.0	210.4	200.7	203.0
	N-7	248.7	265.5	264.2	261.7	249.6
	N-9	162.7	136.3	135.9	146.6	147.8

[a] The chemical shifts are in ppm. The last digit in the ^{1}H chemical shift observed in solvent is placed in parentheses because their chemical shift values can be distinguished only when they appear in the same spectrum. All structures were optimized before calculations of chemical shifts.

and N-9 tautomers of purine derivatives (*21*, *33*). Furthermore, the relative ^{15}N and ^{1}H chemical shift values of the N-7H and N-9H groups in the two tautomers are also qualitatively correct.

These results are encouraging because the requirements for accuracy should be less demanding when the calculations are performed to predict the chemical shift differences between the same molecule under different perturbations than on different molecules. Thus, we extended the calculations to model systems that simulate more realistically the two environments of N-7H Hx in our NMR measurements: in DMSO solution and in the PNP active site (models c and d in Chart 1). Calculations agree well with the experimental observations. In model c, two DMSO molecules are complexed to N-7H Hx tautomer, and the geometries of the complexes were first optimized at the B3LYP/6-31(d,p) level; then the chemical shift calculations were carried out at the B3LYP/6-311(d,p) level so that the results can be compared with those from the water complexes. In model d, the PNP

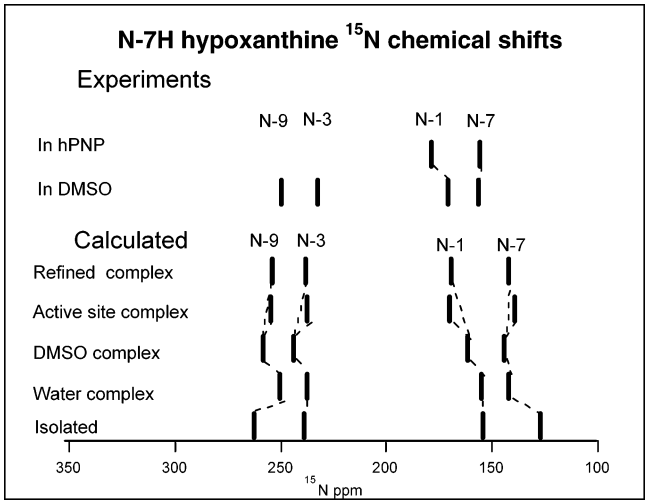

FIGURE 4: Comparison between observed and calculated ^{15}N chemical shifts for Hx under the indicated conditions. The isolated complex was calculated in a vacuum, the water complex is as shown in Chart 1a, the DMSO complex is as shown in Chart 1c, the active site complex is as in Chart 1d, taken from PDB file 1A9R, and the refined active site complex has the H-bond to N-7 shortened by 0.13 Å from that shown in Chart 1d. N-3 and N-9 are remote from catalytic site contacts, and their chemical shifts were not measured in this study.

active site complex was modeled on the basis of the X-ray structure of bovine PNP·Hx (*34*) with three hydrogen-bonding contacts: the C═O group of a $HCONH_2$ molecule hydrogen bonded to the N-7H of Hx to model the contact from the active site Asn243, a water hydrogen bonded to O6, and the COO^- group of a $HCOO^-$ molecule hydrogen bonded to the N-1H of Hx to model the contact from the active site Glu201. For this molecular model, the two oxygen atoms hydrogen bonded to NHs of Hx and the water oxygen were fixed at positions as determined in the X-ray structure [PDB code 1A9R (Chart 1) (*34*)], and the rest of the atomic positions were optimized at the B3LYP/6-31(d,p) level. The chemical shift calculations were then performed on this partially optimized system at the B3LYP/6-311(d,p) level.

Chemical Shifts for Hx Tautomers. The ^{15}N and ^{1}H chemical shifts of the N and NH groups for the N-7H Hx tautomer observed in the experiments and calculated in several model systems are shown in Chart 1 and Figures 4 and 5. The dashed lines in these figures indicate how each of the ^{1}H or ^{15}N chemical shifts are expected to change when the N-7H tautomer of Hx is transferred from gas phase to water, to DMSO, and to the active site of PNP, as predicted by the ab initio chemical shift calculations described above.

Solvent Hydrogen Bond Strengths Agree with ab Initio Calculations. These calculations predict that the ^{1}H and ^{15}N chemical shifts of a NH group would experience downfield shifts when transferred from water to DMSO (Figures 4 and 5). It is well-known that the dielectric constant is not directly proportional to solvent hydrogen-bonding ability either as a donor or as an acceptor (*35*). Another set of empirical parameters for hydrogen bond interactions, which is based on the enthalpy measurements of the electron pair donors with $SbCl_5$ in a dilute solution of dichloroethane, namely, electron pair donor number (DN), has been determined for several solvents and was well correlated with the nucleophilic and hydrogen bond acceptor properties (*35*). DN for DMSO is 29.8, significantly larger than that of water, 18.0. Accord-

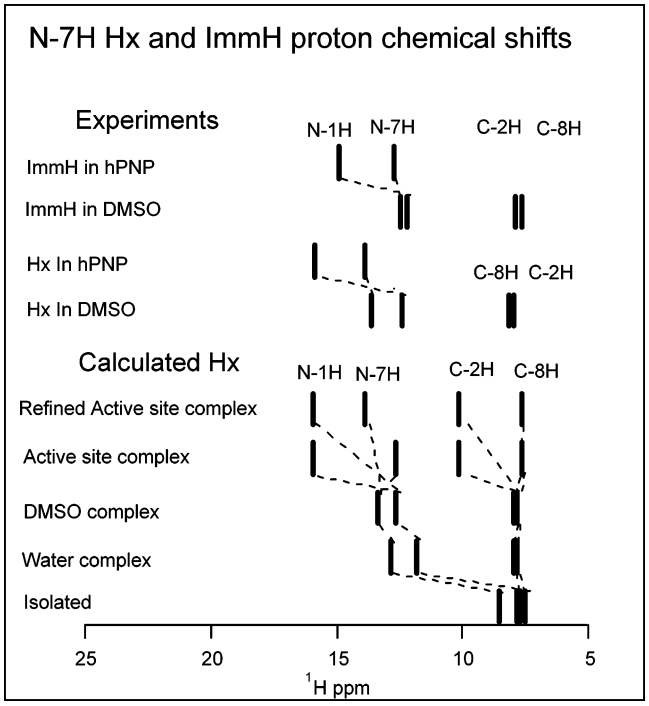

FIGURE 5: Comparison between observed and calculated ^{1}H chemical shifts of Hx under indicated conditions. The lines for ImmH in DMSO and ImmH in hPNP are proton NMR chemical shifts from ImmH in 55% DMSO/45% acetonitrile and from the complex with the transition state analogue ImmH (hPNP·ImmH·PO_4), respectively (*16*); K_d for ImmH for the hPNP complex is approximately 50 pM (*42*). The conditions for computing the chemical shifts are the same as indicated in the legend to Figure 4.

ing to DN theory, when interacting with NH/OH groups, DMSO should form stronger hydrogen bonds than water. Consistent with both empirical DN theory and the ab initio chemical shift calculations of Hx NH groups presented here, we have found the ^{1}H and ^{15}N chemical shifts of the N-7H group of [^{15}N-7]ImmH are downfield shifted by 1 and 2 ppm, respectively, in DMSO compared to that in water in a previous NMR study (*16*).

Chemical Shifts of Hx at the Catalytic Site of hPNP. The calculated ^{1}H and ^{15}N chemical shifts for the N-1H group agree well with experimental observations when Hx is transferred from DMSO to PNP. However, the calculated chemical shifts for the N-7H group change upfield, opposite to the experimental observations (Figures 4 and 5). Additional calculations on N-7H Hx complexed with each of the hydrogen-bonding partners in model d (Chart 1) suggest that the hydrogen bonding on N-1H by the COO^- group not only causes large downfield ^{1}H and ^{15}N chemical shifts of the N-1H group but also causes upfield shifts in both ^{1}H and ^{15}N of the N-7H group. The active site water molecule reduces the effects of COO^- on the chemical shifts of the NH groups slightly; thus it is not a major contributor to the chemical shifts observed for the N-7H group. Since a water molecule hydrogen bonded to an NH group has only minor effects on the chemical shifts of the remote NH group (Table 1), it should be possible to refine the positions of the hydrogen-bonding partners of Hx in model d to fit the experimentally observed chemical shift changes of Hx from DMSO to PNP. In iterative calculations, the distance between N-7 of Hx and its hydrogen-bonded oxygen of $HCONH_2$ was varied from 2.88 to 2.75 Å to refine the active site model complex in terms of chemical shifts. Only the ^{1}H and ^{15}N chemical shifts of the N-7H group are significantly affected by this change. Good agreement was obtained between calculations and experiments for ^{1}H and ^{15}N chemical shift changes for Hx binding to PNP (Figures 4 and 5).

DISCUSSION

Tautomeric Forms of Hypoxanthine in Solution. On the basis of the ^{13}C NMR studies of hypoxanthine in DMSO, the ratio of N-7H and N-9H tautomers has been reported to be 58:42 (*32*). These values agree well with our ratio of 55:45, obtained with slightly different sample conditions. This ratio corresponds to an energy difference of only about 0.1 kcal/mol in favor of N-7H tautomer. Ab initio calculations on the gas phase tautomers, the water complex, or in DMSO indicate that the energy differences between the two tautomers are less than 1 kcal/mol in favor of the N-7H tautomer, in good agreement with experimental determinations.

General Considerations in the Proton Chemical Shift Calculations with ab Initio Methods. de Dios et al. have shown that it is possible to extract protein structural information from NMR data by ab initio ^{13}C, ^{15}N, and ^{1}H chemical shift calculations (*18*). Further efforts in this field have been mostly concentrated on the calculations of ^{13}C and ^{15}N chemical shifts (cf. refs *17* and *19*). The effects of molecular structure and environment on the chemical shift values of CH and OH protons in small molecules have also been studied using ab initio proton chemical shift calculations (*29*, *31*, *36*, *37*). Recently, it has been shown that it is possible to accurately calculate the proton chemical shift of a NH/OH group involved in short, strong hydrogen bonding (*22*). Here, we demonstrate that under specific conditions, with good chemical models, proton chemical shift calculations based on ab initio methods also yield quantitative information about the enzyme−ligand interactions. The NH proton chemical shift change from solution to the PNP-bound state for a small, rigid molecule such as Hx can be reasonably reproduced by ab initio chemical shift calculations. The model systems must include a sufficient number of molecules in direct hydrogen bond contact with Hx. The calculated Hx ^{1}H chemical shift values of the solution state and PNP-bound state are in good agreement with the experimental observation. The calculated ^{15}N chemical shifts of the four nitrogens of Hx have larger discrepancies (Figure 4). Some of these discrepancies are due to systematic errors and can be removed by using a linear scaling procedure when converting the calculated chemical shielding tensor to chemical shift values (*18*, *22*, *29*, *31*). For proton chemical shift values, the linear scaling factor for aromatic CH protons was determined to be 0.984 (*31*). When ^{1}H chemical shifts of NH/OH groups were included, the scaling factor was determined to be ∼0.95 for a much wider chemical shift range [up to ∼21 ppm (*22*)]. Thus, even without the scaling procedure, the calculated ^{1}H chemical shift values should be similar to that of the observed values, in agreement with our studies (Figure 5). The scaling factors for ^{15}N chemical shift were found to be between 0.87 and 0.92 for valines in staphylococcal nuclease, depending on the theory used in the calculations (*18*). Thus, the calculated ^{15}N chemical shift changes should be reduced by about 10% when compared with experimental data. Since we had only a very limited

number of data points, no attempt was made to determine a scaling factor.

Hydrogen-Bonding Interaction on N-1H in the hPNP·Hx Complex. NMR studies establish that the most downfield resonance of the hPNP·Hx complex at 15.9 ppm is due to N-1H (Figure 3). Compared with its value in DMSO, the N-1H resonance is downfield shifted by ~3.5 ppm, suggesting a stronger hydrogen bond to N-1H in the PNP complex. Ab initio calculations indicate that the interaction between N-1H and the carboxyl group of active site Glu201 at the distance determined from X-ray crystallography is sufficient to cause this ^{1}H chemical shift change. This appears to be the only interaction required for the observed ^{1}H chemical shift changes on transfer of the Hx N-1H from solvent (DMSO) to the catalytic site of hPNP.

In a previous NMR study, the ^{1}H chemical shift of N-1H of ImmH in the hPNP·ImmH·PO_4 complex (a transition state analogue) was shifted downfield by ~2.5 ppm relative to that in DMSO solution. X-ray crystal structure studies showed that the distance between the Hx N-1 and the Glu201 oxygen in the bovine PNP·Hx complex was 2.8 Å (*34*), while it was 2.9 Å in the bovine PNP·ImmH·PO_4 complex (*4*). At a crystallographic resolution of 1.5−2.0 Å, this difference is not significant. However, if 0.1 Å difference between the Asn243 oxygen and the N7 of bound Hx or ImmH does occur in hPNP, it correlates to about a 1 ppm N-1H proton chemical shift difference. Previous studies have indicated correlations between proton chemical shifts and hydrogen-bonding distances for O—H- - -O and N—H- - -O hydrogen bonds (*10*, *14*, *38*). Our NMR and the X-ray structure results of PNP·Hx and PNP·ImmH do not agree numerically with the correlation with N—H- - -O hydrogen bonds found in the weak peptide interactions (*38*). The ab initio methods presented here provide a useful approach to cover a wider range of the N−H chemical shift and hydrogen-bonding distances.

Hydrogen-Bonding Interaction on N-7H in hPNP·Hx. The N-7H resonance of bound Hx shifts downfield by ~0.2 ppm, and the ^{15}N-7 resonance shifts upfield by about 0.2 ppm, compared with their values in organic solvent (Figures 1 and 3, Table 1). These results would normally be interpreted as similar hydrogen bond strengths at the N-7H in the hPNP·Hx complex and in the solvent. However, the ab initio chemical shift calculations provide an alternative explanation. The negatively charged Glu201 COO^- group not only induces downfield chemical shift change at its hydrogen-bonding partner N-1H but also induces an upfield shift on the ^{1}H and ^{15}N chemical shifts of the remote N-7H. The local hydrogen bonding at N-7H is stronger than indicated by the local chemical shift induced by the Asn243 carbonyl oxygen. The upfield chemical shifts due to remote COO^- hydrogen bonding at N-1H must be included in the overall change observed by NMR. Such results suggest that, in order to reproduce the experimentally observed chemical shifts of the N-7H in the presence of the hydrogen bonding on N-1H by the COO^- group, the N—7- - -O hydrogen bond distance needs to be shortened by about 0.05 Å. Therefore, our model calculations based on ab initio chemical shift calculations suggest that the hydrogen bonding to the N-7H group is stronger in the PNP·Hx complex than indicated by its chemical shifts, where the experimental ^{1}H and ^{15}N chemical shift values are little changed from their solution values.

Scheme 2: Immucillin-H Transition State Analogue for PNP[a]

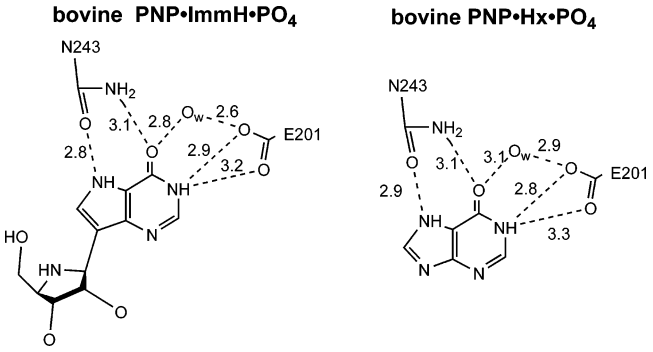

[a] Catalytic site contacts to the 9-deazahypoxanthine in the bovine PNP·ImmH·PO_4 complex are compared to those for the bovine PNP·Hx·PO_4 complex (*4*, *34*). Human PNP is 86% identical with bovine PNP.

While the above conclusion is likely correct, some fine adjustment on the predicted hydrogen-bonding distances to N1H and N7H may be required when more experimental data become available. For example, with the current model, active site contacts are also predicted to induce a downfield ^{1}H chemical shift change of C-2H (~2 ppm), primarily due to its interaction with the other oxygen of the COO^- group. However, since this oxygen is in the same plane as Hx in our model, not out of the plane as shown in the crystal structure, and since other active site interactions with this oxygen are not modeled in our calculations, its effect on the C-2H proton chemical shift is likely to be overestimated in our calculations. Work is in progress to determine the chemical shifts for C-2H, C-8H, and ^{15}N-3 so that the active site contacts can be further refined by ab initio calculations.

Interpretation of NMR Results for the PNP Reaction. The PNP catalytic reaction involves activation of the Hx leaving group by the H-bond contacts summarized above, generation of the ribooxacarbenium ion by neighboring group interactions, and migration of the C1′ of the ribosyl group to a fixed phosphate nucleophile that is activated by catalytic site contacts (*39*, *40*). The tightly bound complex of PNP·ImmH·PO_4 (Scheme 2) resembles the transition state. Mammalian PNPs demonstrate an unusual affinity for Hx in the absence of PO_4 or α-D-ribose-1-PO_4, and this is proposed to result from retention of transition state interactions to Hx that are released only with cooperation from the PO_4 binding pocket (*5*). Tight-binding interactions are apparent both for Hx and for ImmH in the proton NMR measurements (Figure 5). Proton chemical shifts for bound ImmH and Hx both closely resemble the proton chemical shifts calculated for the refined active site complex with Hx only. It is notable that these proton NMR signatures differ significantly for all other states of Hx but closely resemble each other. The chemical shift signature for these complexes is determined by the catalytic site environment, dominated by transition state leaving group interactions. Transition state analogue binding specificity has demonstrated that binding interactions to the purine ring are cooperative. Altering the 6-O to a H-bond donor or altering the pK_a of N-7 to prevent H-bonding to Asn243 decreases binding affinity by 7−10 kcal/mol (*41*). The H-bonds to N-1 and N-7 cannot be energetically isolated because of the cooperative interaction. The NMR results provided here support this cooperative binding ensemble.

SUMMARY AND CONCLUSIONS

Proton chemical shifts are the most sensitive indicator of H-bond environments but have not been exploited widely in ab initio approaches to probe enzyme catalytic site complexes quantitatively, partly due to computational cost (*22*). A combination of solution and on-enzyme experimental spectra for Hx and ImmH bound to mammalian PNP provides an opportune system to explore the feasibility for computational interpretation of ^{1}H chemical shifts. Our results presented here clearly show that the experimental ^{1}H chemical shift values can be interpreted quantitatively in terms of hydrogen-bonding distances by including both local and long-range electrostatic perturbations in the calculation models. Our studies demonstrated that the combined use of NMR and ab initio chemical shift calculations is a powerful approach for the detailed understanding of the enzyme−ligand interactions and has the potential to become a high-resolution tool for structural determination. Cooperative binding interactions to the purine leaving group are well documented from transition state analogue specificity studies. The PNP·Hx complex refined here clearly retains features of transition state interactions by making cooperative and cumulative hydrogen bonds to both N-7H and N-1H of Hx.

REFERENCES

1. Stoeckler, J. D. (1984) in *Developments in Cancer Chemotherapy* (Glazer, R. J., Ed.) pp 35−60, CRC Press, Boca Raton, FL.
2. Bzowska, A., Kulikowska, E., and Shugar, D. (2000) Purine nucleoside phosphorylases: properties, functions, and clinical aspects, *Pharmacol. Ther. 88*, 349−425.
3. Mazzella, L. J., Parkin, D. W., Tyler, P. C., Furneaux, R. H., and Schramm, V. L. (1996) Mechanistic diagnoses of N-ribohydrolases and purine nucleoside phosphorylase, *J. Am. Chem. Soc. 118*, 2111−2112.
4. Fedorov, A., Shi, W., Kicska, G., Fedorov, E., Tyler, P. C., Furneaux, R. H., Hanson, J. C., Gainsford, G. J., Larese, J. Z., Schramm, V. L., and Almo, S. C. (2001) Transition state structure of purine nucleoside phosphorylase and principles of atomic motion in enzymatic catalysis, *Biochemistry 40*, 853−860.
5. Kline, P. C., and Schramm, V. L. (1992) Purine nucleoside phosphorylase. Inosine hydrolysis, tight binding of the hypoxanthine intermediate, and third-the-sites reactivity, *Biochemistry 31*, 5964−5973.
6. Lin, J., Westler, W. M., Cleland, W. W., Markley, J. L., and Frey, P. A. (1998) Fractionation factors and activation energies for exchange of the low barrier hydrogen bonding proton in peptidyl trifluoromethyl ketone complexes of chymotrypsin, *Proc. Natl. Acad. Sci. U.S.A. 95*, 14664−14668.
7. Frey, P. A., Whitt, S. A., and Tobin, J. B. (1994) A low-barrier hydrogen bond in the catalytic triad of serine proteases, *Science 264*, 1927−1930.
8. Markley, J. L., and Westler, W. M. (1996) Protonation-state dependence of hydrogen bond strengths and exchange rates in a serine protease catalytic triad: bovine chymotrypsinogen A, *Biochemistry 35*, 11092−11097.
9. Gerlt, J. A., Kreevoy, M. M., Cleland, W., and Frey, P. A. (1997) Understanding enzymic catalysis: the importance of short, strong hydrogen bonds, *Chem. Biol. 4*, 259−267.
10. Mildvan, A. S., Harris, T. K., and Abeygunawardana, C. (1999) Nuclear magnetic resonance methods for the detection and study of low-barrier hydrogen bonds on enzymes, *Methods Enzymol. 308*, 219−245.
11. Wei, Y., and McDermott, A. E. (1999) in *Modeling NMR Chemical Shifts: gaining insights into structure and environment* (Facelli, J. C., and deDios, A. C., Eds.) pp 177−193, Oxford University Press, Oxford.
12. Halkides, C. J., Wu, Y. Q., and Murray, C. J. (1996) A low-barrier hydrogen bond in subtilisin: ^{1}H and ^{15}N NMR studies with peptidyl trifluoromethyl ketones, *Biochemistry 35*, 15941−15948.
13. Loh, S. N., and Markley, J. L. (1994) Hydrogen bonding in proteins as studied by amide hydrogen D/H fractionation factors: application to staphylococcal nuclease, *Biochemistry 33*, 1029−1036.
14. Zhao, Q., Abeygunawardana, C., Gittis, A. G., and Mildvan, A. S. (1997) Hydrogen bonding at the active site of delta 5−3-ketosteroid isomerase, *Biochemistry 36*, 14616−14626.
15. Kreevoy, M. M., and Liang, T. M. (1980) Structures and isotopic fractionation factors of complexes, A1HA2-, *J. Am. Chem. Soc. 102*, 3315−3322.
16. Deng, H., Lewandowicz, A., Cahill, S. M., Furneaux, R. H., Tyler, P. C., Girvin, M. E., Callender, R. H., and Schramm, V. L. (2004) Assignment of downfield proton resonances in purine nucleoside phosphorylase·immucillin-H complex by saturation-transferred NOEs, *Biochemistry 43*, 1980−1987.
17. Facelli, J. (2004) Calculations of chemical shieldings: Theory and applications, *Concepts Magn. Reson., Part A 20A*, 42−69.
18. de Dios, A. C., Pearson, J. G., and Oldfield, E. (1993) Secondary and tertiary structural effects on protein NMR chemical shifts: an ab initio approach, *Science 260*, 1491−1496.
19. Facelli, J. C., and de Dios, A. C., Eds. (1999) *Modeling NMR chemical shifts: gaining insights into structure and environment*, American Chemical Society, Washington, DC, (distributed by Oxford University Press, New York).
20. Hu, J. Z., Facelli, J. C., Alderman, D. W., Pugmire, R. J., and Grant, D. M. (1998) ^{15}N Chemical Shift Tensors in Nucleic Acid Bases, *J. Am. Chem. Soc. 120*, 9863−9869.
21. Laxer, A., Major, D. T., Gottlieb, H. E., and Fischer, B. (2001) (^{15}N5)-Labeled adenine derivatives: synthesis and studies of tautomerism by ^{15}N NMR spectroscopy and theoretical calculations, *J. Org. Chem. 66*, 5463−5481.
22. Westler, W. M., Weinhold, F., and Markley, J. L. (2002) Quantum chemical calculations on structural models of the catalytic site of chymotrypsin: comparison of calculated results with experimental data from NMR spectroscopy, *J. Am. Chem. Soc. 124*, 14373−14381.
23. Abad, J. L., Gaffney, B. L., and Jones, R. A. (1999) ^{15}N-Multilabeled adenine and guanine nucleosides. Syntheses of [1,3,-NH(2)−(15)N(3)]- and [2-(13)C-1,3,NH(2)−(15)N(3)]-labeled adenosine, guanosine, 2′-deoxyadenosine, and 2′-deoxyguanosine, *J. Org. Chem. 64*, 6575−6582.
24. Shallop, A. J., Gaffney, B. L., and Jones, R. A. (2003) Use of ^{13}C as an indirect tag in ^{15}N specifically labeled nucleosides. Syntheses of [8-^{13}C-1,7,NH2−^{15}N3]adenosine, -guanosine, and their deoxy analogues, *J. Org. Chem. 68*, 8657−8661.
25. Plateau, P., and Gueron, M. (1982) Exchangeable proton NMR without base-line distortion, using new strong-pulse sequences, *J. Am. Chem. Soc. 104*, 7310−7311.
26. Deng, H., Cahill, S., Kurz, L., and Callender, R. (2004) The assignment of downfield proton resonances in an enzyme inhibitor complex using time-dependent saturation transferred NOEs, *J. Am. Chem. Soc. 126*, 1952−1953.
27. Pervushin, K., Riek, R., Wider, G., and Wuthrich, K. (1997) Attenuated T2 relaxation by mutual cancellation of dipole−dipole coupling and chemical shift anisotropy indicates an avenue to NMR structures of very large biological macromolecules in solution, *Proc. Natl. Acad. Sci. U.S.A. 94*, 12366−12371.
28. Frisch, M. J., Trucks, G. W., Head-Gordon, M., Gill, P. M. W., Wong, M. W., Foresman, J. B., Johnson, B. G., Schlegel, H. B., Robb, M. A., Replogle, E. S., Gomperts, R., Andres, J. L., Raghavachari, K., Binkley, J. S., Gonzalez, C., Martin, R. L., Fox, D. J., Defrees, D. J., Baker, J., Stewart, J. J. P., and Pople, J. A. (1998) *Gaussian 98*, Gaussian, Inc., Pittsburgh, PA.
29. Rablen, P. R., Pearlman, S. A., and Finkbiner, J. (1999) A comparison of density functional methods for the estimation of proton chemical shifts with chemical accuracy, *J. Phys. Chem. A 103*, 7357−7363.
30. Wang, B., Miskolizie, M., Kotovych, G., and Pulay, P. (2002) Backbone structure confirmation and side chain conformation refinement of a bradykinin mimic BKM-824 by comparing calculated (1)H, (13)C and (19)F chemical shifts with experiment, *J. Biomol. Struct. Dyn. 20*, 71−80.
31. Wang, B., Hinton, J. F., and Pulay, P. (2002) Accurate prediction of proton chemical shifts. II. Peptide analogues, *J. Comput. Chem. 23*, 492−497.
32. Chenon, M. T., Pugmire, R. J., Grant, D. M., Panzica, R. P., and Townsend, L. B. (1975) Carbon-13 magnetic resonance. XXVI. Quantitative determination of the tautomeric populations of certain purines, *J. Am. Chem. Soc. 97*, 4636−4642.

33. Marek, R., Brus, J., Touek, J., Kovács, L., and Hocková, D. (2002) N7- and N9-substituted purine derivatives: a ^{15}N NMR study, *Magn. Reson. Chem. 40*, 353−360.
34. Koellner, G., Luic, M., Shugar, D., Saenger, W., and Bzowska, A. (1997) Crystal structure of calf spleen purine nucleoside phosphorylase in a complex with hypoxanthine at 2.15 Å resolution, *J. Mol. Biol. 265*, 202−216.
35. Gutmann, V. (1978) *The Donor−Acceptor Approach to Molecular Interactions*, Plenum Press, New York.
36. Martin, N. H., Allen, N. W., III, and Moore, J. C. (2000) An algorithm for predicting the NMR shielding of protons over substituted benzene rings, *J. Mol. Graphics Modell. 18*, 242−246.
37. Lampert, H., Mikenda, W., Karpfen, A., and Kählig, H. (1997) NMR shieldings in benzoyl and 2-hydroxybenzoyl compounds. Experimental versus GIAO calculated data, *J. Phys. Chem. A 101*, 9610−9617.
38. Wagner, G., Pardi, A., and Wuethrich, K. (1983) Hydrogen bond length and proton NMR chemical shifts in proteins, *J. Am. Chem. Soc. 105*, 5948−5949.
39. Schramm, V. L., and Grubmeyer, C. (2004) Phosphoribosyltransferase mechanisms and roles in nucleic acid metabolism, *Prog. Nucleic Acid Res. Mol. Biol. 78*, 261−304.
40. Deng, H., Lewandowicz, A., Schramm, V. L., and Callender, R. (2004) Activating the phosphate nucleophile at the catalytic site of purine nucleoside phosphorylase: a vibrational spectroscopic study, *J. Am. Chem. Soc. 126*, 9516−9517.
41. Kicska, G. A., Tyler, P. C., Evans, G. B., Furneaux, R. H., Shi, W., Fedorov, A., Lewandowicz, A., Cahill, S. M., Almo, S. C., and Schramm, V. L. (2002) Atomic dissection of the hydrogen bond network for transition-state analogue binding to purine nucleoside phosphorylase, *Biochemistry 41*, 14489−14498.
42. Lewandowicz, A., and Schramm, V. L. (2004) Transition state analysis for human and *Plasmodium falciparum* purine nucleoside phosphorylases, *Biochemistry 43*, 1458−1468.

BI048167I